



Cite this: DOI: 10.1039/c8nj00281a

# Nickel(II) riboflavin complex as an efficient nanobiocatalyst for heterogeneous and sustainable oxidation of benzylic alcohols and sulfides

 Ravak Hasanpour, Fahimeh Feizpour,  Maasoumeh Jafarpour \* and Abdolreza Rezaeifard \*

In this paper, a novel nickel–riboflavin nanocomplex has been prepared *via* the incorporation of Ni(OAc)<sub>2</sub> with riboflavin. This new heterogeneous nanocatalyst showed high catalytic activity towards green oxidation reactions. The structural and morphological characterization of the as-prepared nanocomplex was carried out using different techniques such as FT-IR, ICP-AES, TGA, SEM, EDX, TEM, UV-vis and elemental analysis. The nano-biocatalyst showed high oxidation stability and desired activity in the aerobic benzylic oxidation of a structurally diverse set of alcohols in ethyl acetate as a safe solvent. Further, oxidation of sulfides in the presence of H<sub>2</sub>O<sub>2</sub> was successfully achieved, producing the corresponding sulfoxides in high yields and with excellent selectivity. The facile and practical reusability of the solid catalyst at the end of the reaction was also observed.

Received 17th January 2018,  
Accepted 30th March 2018

DOI: 10.1039/c8nj00281a

rsc.li/njc

## 1. Introduction

Nowadays, advancing catalytic technologies towards sustainable approaches for the conversion of raw materials into fine chemicals, high-value building blocks and synthetic applications represents a grand challenge that must be urgently addressed due to growing environmental concerns.<sup>1–5</sup> Further, achieving the goals of green chemistry is a strong incentive, and will offer indispensable tools to improve environmental and economic issues. Therefore, the synthesis of robust, readily available, active, multi-functional and benign catalysts is a highly cherished goal for researchers.<sup>6,7</sup> Moreover, it is extremely desirable that the catalytic protocols involved are energy efficient, economically viable, operationally simple, and environmentally friendly. To achieve this goal, suitable synthetic routes based on naturally sourced catalysts must be developed.

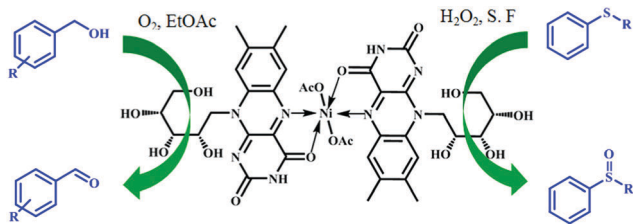
Riboflavin (Rf), or vitamin B<sub>2</sub>, is an eco-friendly, naturally occurring important biological redox cofactor, which is essential for human and animal health.<sup>8</sup> Besides the biological relevance of Rf, this molecule acts as a photosensitizer in the photo-oxidation of a range of contaminants.<sup>9</sup> Riboflavin, especially flavin,<sup>10</sup> possesses unrivaled properties, such as improved activity, selectivity, photochemical stability and environmental protection, and is regarded as a promising catalyst owing to its varied applications,

including photo-oxidation and reduction,<sup>11,12</sup> oxidative esterification, amidation of aldehydes,<sup>13</sup> oxidation of myoglobin<sup>14</sup> and electrochemical properties.<sup>15</sup> Although Rf has been reported as an organocatalyst, few reports have explored the catalytic activity of Rf nanocomplexes in synthetic organic reactions.<sup>16,17</sup>

Oxidative transformations, especially selective oxidation (selox) reactions,<sup>18</sup> possess some desired features of a 'green' procedure, in terms of reduced waste production, and play pivotal roles in the chemical industry.<sup>19–22</sup> However, despite extensive research in which notable efficiencies have been demonstrated for a broad array of oxidative transformations, most of these traditional protocols rely on the use of hazardous terminal oxidants or cause the generation by-products.<sup>23–26</sup> In fact, there is still an evident need for methodological improvements of selox reactions based on green reagents and solvents. Today, a clean and environmentally friendly process using environmentally benign oxidants such as oxygen,<sup>27–31</sup> air,<sup>32–36</sup> or hydrogen peroxide<sup>37–40</sup> is preferred.

In view of the above and in a continuation of our studies to develop innovative strategies for the selective catalytic aerobic oxidation of organic compounds,<sup>41–47</sup> herein, we wish to present an efficient and sustainable aerobic oxidative nanobiocatalyst, synthesized *via* the complexation of Ni(II) with riboflavin under ultrasound agitation. The catalyst was used in the efficient, environmentally-friendly and selective aerobic oxidation of benzylic alcohols to aldehydes in ethyl acetate as a safe solvent. It was also used in the selective oxidation of sulfides in the presence of H<sub>2</sub>O<sub>2</sub> under solvent free conditions (Scheme 1).

Catalysis Research Laboratory, Department of Chemistry, Faculty of Science, University of Birjand, Birjand, 97179-414, Iran. E-mail: mjafarpour@birjand.ac.ir, rrezaeifard@birjand.ac.ir, rrezaeifard@gmail.com



Scheme 1 The selective oxidation performance of the Ni(II)Rf<sub>2</sub> nanocomplex.

Moreover, the nanocomplex was demonstrated to be scalable, in terms of both the catalyst synthesis and its implementation.

## 2. Experimental

### 2.1. General remarks

All chemicals were purchased from Merck and Fluka Chemical Companies. The FT-IR spectra were recorded on a NICOLET system. The TGA measurements were obtained on a TGA-50 (Shimadzu) at a heating rate of 10 °C min<sup>-1</sup> under 20 mL min<sup>-1</sup> flowing air. TEM images were obtained using TEM instrumentation 906E (Zeiss, Jena, Germany). Samples for TEM experiments were prepared by dispersing the samples in ethanol, sonicating for 30 min to ensure adequate dispersion of the nanostructures, and evaporating one drop of the solution on 200 mesh form bar-coated copper grids. SEM images were obtained using a TESCAN Vega model. Inductively coupled plasma (ICP) atomic emission spectroscopy was conducted with an OPTIMA 7300DV. UV-vis spectra were recorded on a SPECORD<sup>®</sup> 210 PLUS. Elemental analysis was carried out on an Eager 300 CHNS elemental analyzer. The progress of the reactions was monitored by TLC using silica-gel SIL G/UV 254 plates and also by GC-FID on a Shimadzu GC-16A instrument using a 25 m CBP1-S25 (0.32 mm ID, 0.5 μm coating) capillary column. NMR spectra were recorded on a Bruker Avance DPX 400 MHz instrument.

### 2.2. Fabrication of Ni(II) riboflavin nanocomplex (Ni(II)Rf<sub>2</sub>)

To 0.12 g of riboflavin in ethanol (5 mL), was gradually added 1 mmol Ni(OAc)<sub>2</sub> dissolved in ethanol over a period of 20 min at room temperature under ultrasonic agitation. Then, the as-obtained mixture was kept for 2 h under these conditions. Afterwards, the product was centrifuged and unreacted riboflavin was removed by washing with distilled water and ethanol. Finally, the Ni(II)Rf<sub>2</sub> nanocomplex was obtained after drying for 12 h in air.

### 2.3. General procedure for aerobic oxidation of benzyl alcohols

To a mixture of benzyl alcohol (1 mmol) and Ni(II)Rf<sub>2</sub> nanocomplex (3.1 mol%, 0.005 g) in EtOAc (0.5 mL), was added NHPI (9 mol%, 0.011 g), and the reaction mixture was stirred under air at 70 °C for the required time. The reaction progress was monitored using GC, and the yields of the products were determined using GC and NMR analysis. The pure product was

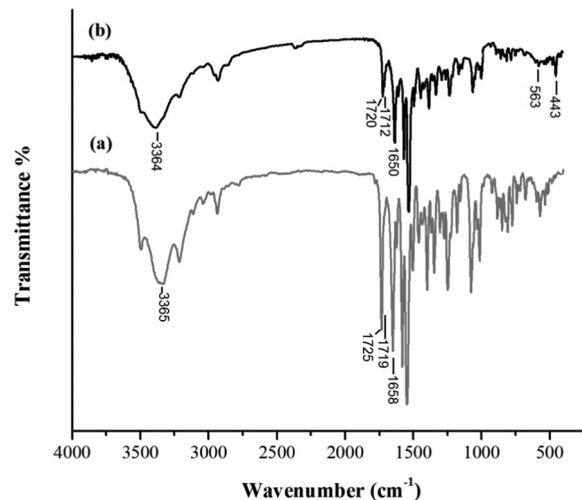


Fig. 1 FTIR spectra of (a) Rf and (b) Ni(II)Rf<sub>2</sub> nanocomplex.

confirmed using plate silica chromatography using *n*-hexane/EtOAc (10:3).

### 2.4. General procedure for oxidation of sulfides

To a mixture of the sulfide (1 mmol) and Ni(II)Rf<sub>2</sub> nanocomplex (3.1 mol%, 0.005 g), was added H<sub>2</sub>O<sub>2</sub> (2 mmol), and the reaction mixture was stirred at 40 °C for the required time. The reaction progress was monitored using TLC, and the yields of the products were determined using GC analysis. After the completion of the reaction, the Ni(II)Rf<sub>2</sub> nanocomplex was extracted by adding ethyl acetate (5 mL) followed by centrifugation and decantation (3 × 5 mL). Then, the desired product (liquid phase) was extracted by plate chromatography eluted with *n*-hexane/EtOAc (10/5).

## 3. Results and discussion

### 3.1. Structural characterization

The FT-IR measurements of the Ni(II)Rf<sub>2</sub> nanocomplex and Rf are depicted in Fig. 1. Comparison of the infrared spectra of Ni(II)Rf<sub>2</sub> with the Rf moiety as a free ligand confirmed the successful complexation. The stretching bands at 1720, 1712 and 1650 cm<sup>-1</sup> are attributed to C=O and C=N in the conjugated system, respectively, which are present in Rf.<sup>48</sup> In Fig. 1b (the FT-IR of the Ni(II)Rf<sub>2</sub> nanocomplex), these frequencies are shifted to lower wavenumbers along with lower intensities, indicating the involvement of C=O and C=N in the complexation. The appearance of a signal at 3364 cm<sup>-1</sup> reveals that the -NH groups of the heterocyclic ring remain unchanged, indicating that there is no metal-to-NH coordination in this complex. Also, broad peaks at around 3200–3500 cm<sup>-1</sup> correspond to free hydroxyl groups. The absorption bands at 443 and 563 cm<sup>-1</sup> can be assigned to the stretching vibrations of the Ni–O and Ni–N bonds, respectively. The peaks between 1000 and 1500 cm<sup>-1</sup> belong to the bending and stretching vibrations of N–H, C–H, C–C and C–O bonds, which are present in the Rf structure.

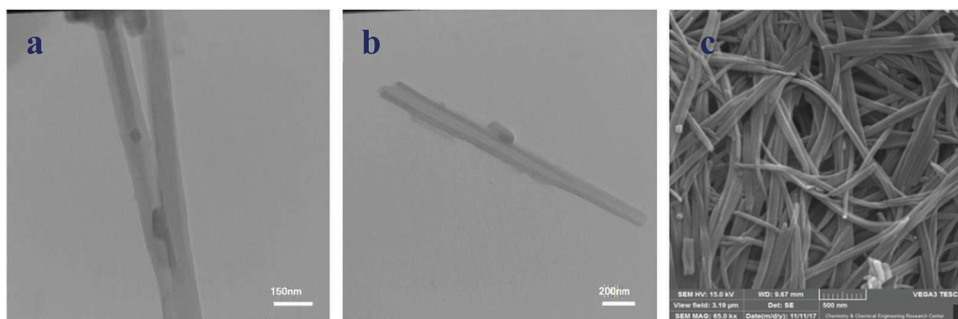


Fig. 2 (a and b) TEM images and (c) SEM micrograph of Ni(II)Rf<sub>2</sub> nanocomplex.

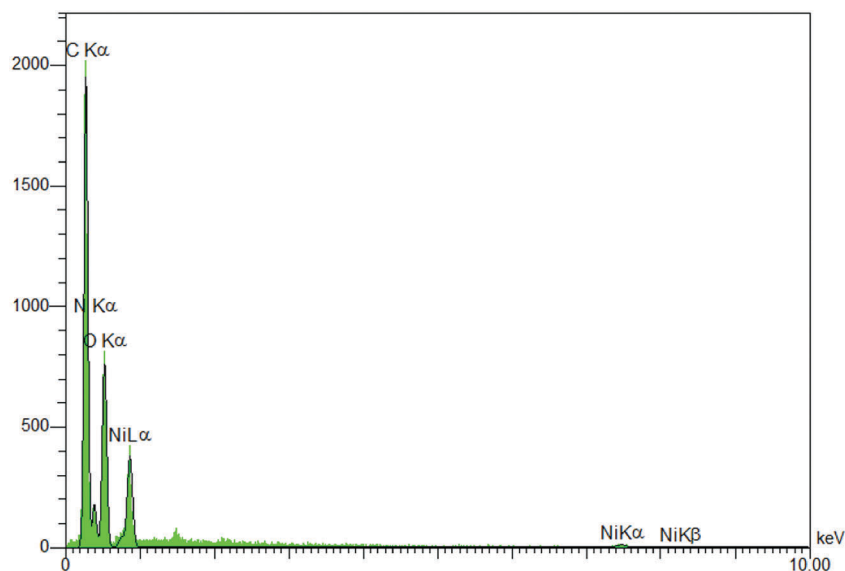


Fig. 3 EDX analysis of Ni(II)Rf<sub>2</sub> nanocomplex.

This region is similar in both Rf and the Ni(II)Rf<sub>2</sub> complex, with just a little displacement.

TEM and SEM observations clearly reveal the nanorod morphology of the prepared nanocomplex, with nanorods of 80–90 nm in diameter and 390–410 nm in length (Fig. 2).

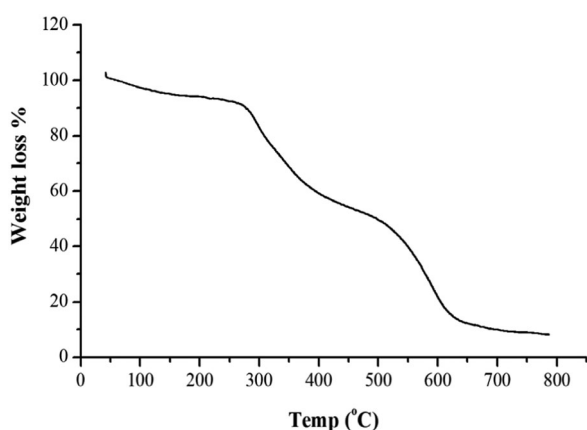


Fig. 4 TGA curve of the Ni(II)Rf<sub>2</sub> nanocomplex.

The obtained SEM image shown in Fig. 2c allows us to verify that the Ni(II)Rf<sub>2</sub> complex exhibits a well-formed nano-rod

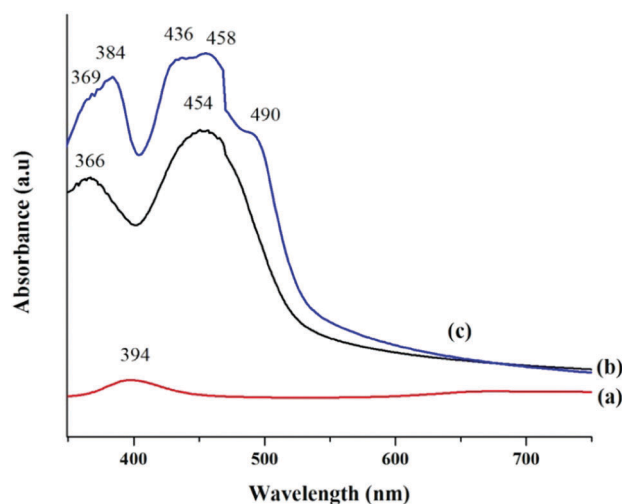


Fig. 5 UV-vis spectra of (a) Ni(OAc)<sub>2</sub>, (b) Rf and (c) Ni(II)Rf<sub>2</sub> nanocomplex (dispersion in ethanol through sonication for 30 min, centrifuging once, and the supernatant is taken to analysis).

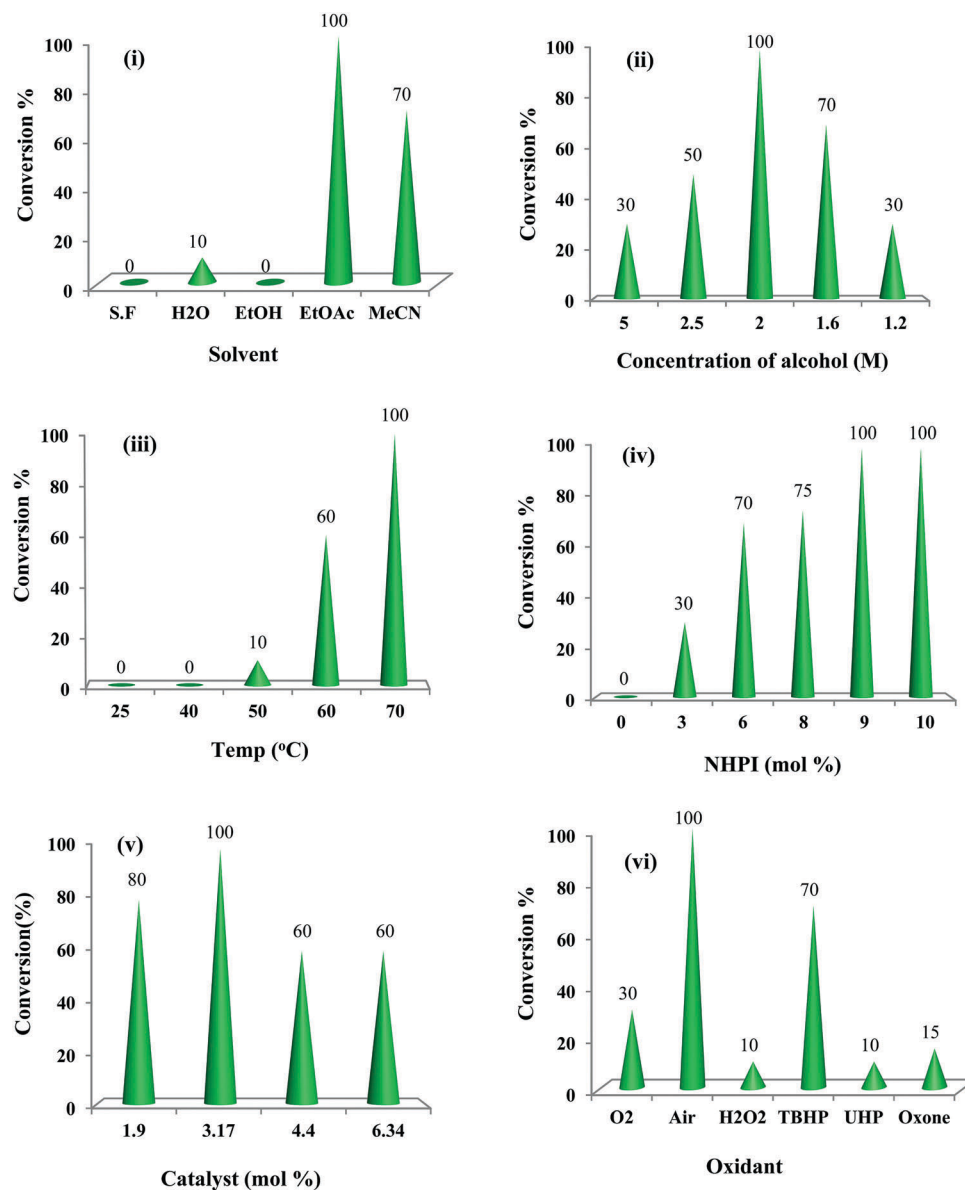


Fig. 6 The screening of the (i) solvent nature, (ii) concentration of alcohol, (iii) temperature, (iv) NHPI, (v) amount of catalyst and (vi) oxidant nature on the oxidation of 4-chlorobenzyl alcohol (1 mmol) catalyzed by Ni(II)Rf<sub>2</sub> after 4 h under air, except for mentioned oxidant in (vi).

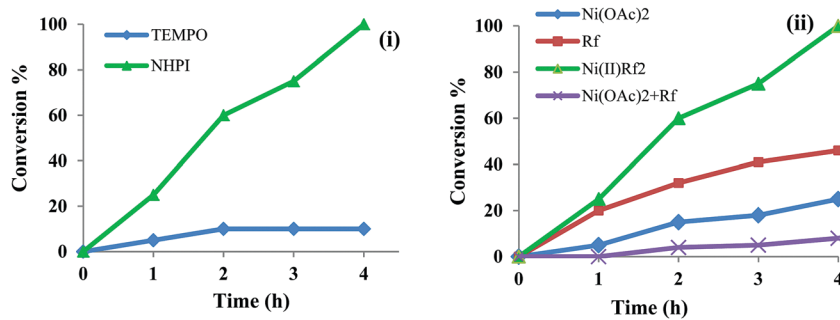


Fig. 7 Comparison of (i) oxidation of 4-chlorobenzyl alcohol (1 mmol) in the presence of NHPI and TEMPO (9 mol%) by Ni(II)Rf<sub>2</sub> nanobiocatalyst at 70 °C under air after 4 h, and (ii) oxidation of 4-chlorobenzyl alcohol (1 mmol) in the presence of NHPI using Ni(OAc)<sub>2</sub>, Rf, Rf + Ni(OAc)<sub>2</sub> and Ni(II)Rf<sub>2</sub> as catalysts at 70 °C under air after 4 h.

shape. Such facts are in agreement with the formation of the new complex.

The presence of the Ni complex was confirmed by ICP-ESA and EDX analysis (Fig. 3). Also, from the ICP-ESA spectroscopy results, the amount of Ni was evaluated to be 7.5 wt%. Therefore, each gram of nanocatalyst contains 1.2 mmol of Ni.

TGA was performed at a heating rate of 10 °C min<sup>-1</sup> in air over a range of 25–800 °C to investigate the thermal behaviour of the Ni(II)Rf<sub>2</sub> nanocomplex (Fig. 4). Accordingly, the first mass loss up until 180 °C corresponds to the dehydration of the sample and the second mass loss in the range of 260–630 °C (58%) is attributed to the complete thermal decomposition of the Rf moiety. These results are in good agreement with the elemental analysis data (calc.: 49.10 C%, 4.99 H%, 12.06 N%; found: 48.98 C%, 5.00 H%, 12.02 N%).

Further evidence for the successful fabrication of the Ni(II)Rf<sub>2</sub> complex was obtained from UV-vis spectroscopy (Fig. 5). Clearly, there are recognizable new bands at 384, 436 and 490 nm for the Ni(II)Rf<sub>2</sub> nanocomplex with some red-shifting of the absorptions resulting from complex formation.<sup>15,16</sup>

### 3.2. Catalytic activities

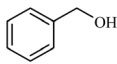
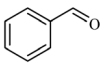
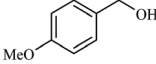
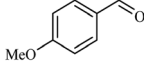
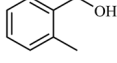
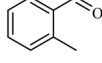
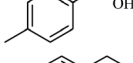
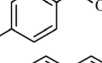
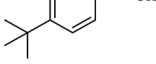
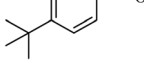
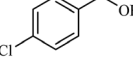
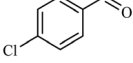
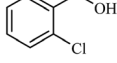
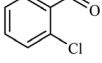
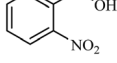
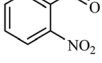
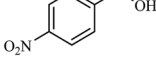
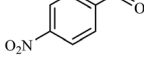
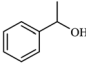
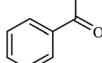
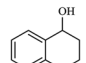
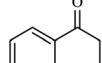
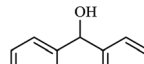
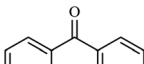
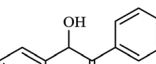
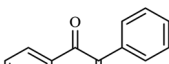
Catalytic experiments were initiated with the oxidation of 4-chlorobenzyl alcohol (1 mmol) under air in the presence of NHPI (*N*-hydroxyphthalimide), knowing that the catalyst-free condition does not have the ability to trigger the reaction under any conditions. Different factors were screened to standardize the reaction conditions, such as the nature and amount of solvent and oxidant, temperature, and the quantity of NHPI or catalyst. The schematic examination for 4-chlorobenzaldehyde yield can be found in Fig. 6.

The data in Fig. 6-i demonstrate the effect of solvent on the catalytic performance. The reaction did not proceed in EtOH or the solvent-free condition, and demonstrated a low conversion in water under air at 70 °C. EtOAc and MeCN resulted in 100% and 70% conversion, respectively. So, EtOAc as a safe solvent was selected. Further investigations demonstrated that a 2 M concentration of alcohol and 70 °C are the best conditions for this oxidation reaction (Fig. 6-ii and iii). The efficiency of oxidation was affected remarkably by the amount of NHPI, indicating that a radical process prevails to a great extent in the present system (Fig. 6-iv).<sup>49</sup> Moreover, replacing NHPI with TEMPO ((2,2,6,6-tetramethylpiperidin-1-yl)oxyl) under the same conditions (Fig. 7-i) reduced the 4-chlorobenzyl alcohol conversion to less than 20%.

Also, a survey of the results shown in Fig. 6-iv revealed that a sufficient amount of catalyst loading of 3.1 mol% led to higher conversion, but this decreased with higher concentrations of catalyst. Based on the data in Fig. 6-vi, common oxidants such as O<sub>2</sub>, H<sub>2</sub>O<sub>2</sub>, TBHP, UHP and Oxon were weaker oxidants than air for this transformation.

The ability of riboflavin, nickel acetate and a combination of riboflavin and nickel acetate to promote the oxidation of 4-chlorobenzyl alcohol was then probed under optimized conditions (Fig. 7-ii). These compounds exhibited poor activity under this condition and the preferable catalytic performance of Ni(II)Rf<sub>2</sub> was confirmed.

Table 1 Oxidation of benzylic alcohols by Ni(II)Rf<sub>2</sub> nanocomplex<sup>a</sup>

Entry	Alcohol	Product <sup>b</sup>	Yield <sup>c</sup> (%) (isolated yield (%))
1			91 (88)
2			83 (79)
3			91 (77)
4			88 (82)
5			89 (81)
6			93 (89)
7			66 (61)
8			20
9			40
10			81 (78)
11			78 (75)
12			73 (70)
13			64 (59)

<sup>a</sup> The molar ratio of substrate/NHPI/catalyst was 10000:9:317. The reactions were run under air, at 70 °C in EtOAc (0.5 mL) for 4 h. <sup>b</sup> The products were identified using <sup>1</sup>H NMR spectroscopy or by comparison with the retention times of authentic samples in GC analysis. <sup>c</sup> The selectivities of the products were >99% based on GC analysis.

Afterwards, with improved procedures for aerobic oxidation in hand, we focused on the evaluation of the substrate scope. Towards this aim, a set of structurally and electronically similar benzylic alcohols was subjected to the catalytic oxidation protocol (Table 1). As shown in Table 1, good to excellent yields were obtained for different primary and secondary benzylic alcohols, except for those with the aryl ring substituted with a nitro group (entries 8 and 9). It should be noted that the selectivity of the procedure was prominent. Therefore, no overoxidation of primary and secondary benzylic alcohols to the corresponding carboxylic acids and ester was observed, respectively.

Next, we evaluated the potential of the title nanocomplex for the selective aerobic oxidation of sulfides. The result obtained

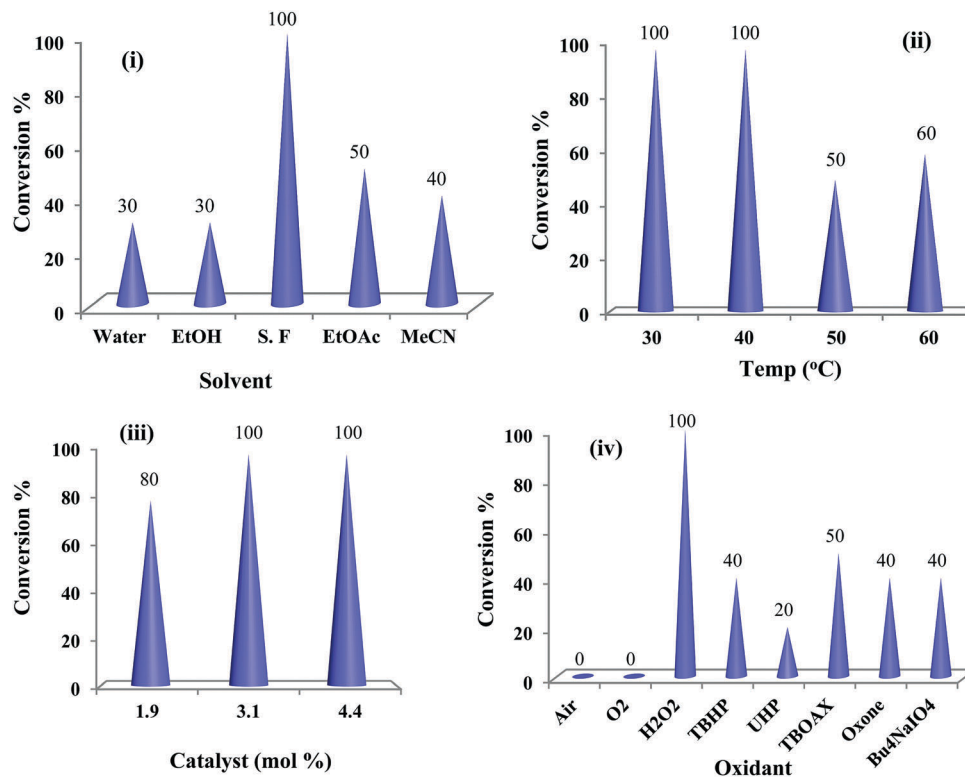


Fig. 8 The screening of the (i) solvent nature, (ii) temperature, (iii) catalyst amount and (iv) oxidant nature on the oxidation of thioanisole (1 mmol) catalyzed by Ni(II)Rf<sub>2</sub> after 1.3 h at 30 °C using H<sub>2</sub>O<sub>2</sub> (2 mmol), except for the mentioned oxidant.

for the oxidation of thioanisole under the optimized conditions of oxidation of benzylic alcohols was disappointing. Therefore, to achieve new conditions for efficient oxidation, several factors were screened (Fig. 8). The best performance of the Ni(II)Rf<sub>2</sub> nanocomplex was achieved in the selective oxidation of thioanisole (1 mmol) in the presence of H<sub>2</sub>O<sub>2</sub> (2 mmol), using 3.1 mol% catalyst and a reaction time of 1.3 h under solvent free conditions.

Additionally, Rf and Ni(OAc)<sub>2</sub>, as well as a combination of Rf and nickel acetate, were tested in the model oxidation reaction under optimized conditions, and both of them demonstrated lower efficiency than the Ni(II)Rf<sub>2</sub> nanocomplex in the sulfoxidation of thioanisole (Rf 10%, Ni(OAc)<sub>2</sub> 30%, Rf + Ni(OAc)<sub>2</sub> 43% yields of sulfoxide).

Then, the generality of this catalytic system was examined with a number of sulfides under optimized conditions and the corresponding sulfoxides were easily produced in good to excellent yields and 100% selectivity (Table 2). It is worth mentioning that no products resulting from benzylic oxidation were detected under this condition (Table 2, entries 3 and 4). The chemoselectivity of the procedure was remarkable. The allylic sulfides were oxidized to the corresponding sulfoxides, whereas the olefine moiety remained completely intact (Table 2, entries 5 and 6)

### 3.3. Reusability of catalyst

The level of reusability and the catalytic activity are imperative factors for the practical application of heterogeneous systems.

In this line, the recovery of the Ni(II)Rf<sub>2</sub> nanocomplex was explored in the aerobic oxidation of 4-chlorobenzyl alcohol and oxidation of thioanisole as blank reactions. After completion of the reactions, the nanocomplex was separated by centrifugation, followed by decantation (3 × 5 mL EtOAc). The recovered catalyst was dried under reduced pressure. In order to test the activity as well as the stability, the catalyst was recycled at least six times. The catalyst gave remarkable results without noticeable loss in catalytic activity, and products were obtained in 93–90% and 96–92% yields for the oxidation of 4-chlorobenzyl alcohol and thioanisole, respectively (Fig. 9). Using ICP-AES measurements, no leaching of Ni was observed for the six recovered catalysts. Furthermore, a comparison of the FT-IR spectra of the used Ni(II)Rf<sub>2</sub> nanocatalyst with those of the fresh catalyst showed that the structure of the catalyst remained almost completely intact after six recovery cycles (Fig. 10).

Since the efficiency of the aerobic oxidation of benzylic alcohols in the present protocol was dependent on the amount of NHPI, the reaction did not proceed in the absence of NHPI under any conditions. Therefore, a radical mechanism may be suggested for the title oxidation system using O<sub>2</sub> according to the literature<sup>50,51</sup> (Scheme 2). This was further supported by reduced oxidation of 4-chlorobenzyl alcohol in the presence of radical scavengers such as 2,6-di-*tert*-butyl-4-methylphenol under the same conditions.

Also, a plausible mechanism has been proposed for the oxidation of sulfides in the presence of H<sub>2</sub>O<sub>2</sub> as an oxidant

Table 2 Sulfides oxidation in presence of Ni(II)Rf<sub>2</sub> nanocomplex<sup>a</sup>

Entry	Sulfide	Product <sup>b</sup>	Time (h)	Conversion (%) (isolated yield) <sup>c</sup>
1			1.3	100 (95)
2			2	60 (56)
3			2	80 (73)
4			2	100 (90)
5			3	90 (81)
6			1.3	100 (95)
7			1	100 (92)
8			2	65 (60)
9			2	100 (90)

<sup>a</sup> Reaction conditions: molar ratio of sulfide/H<sub>2</sub>O<sub>2</sub>/Cat, 10 000 : 20 000 : 317 and the reaction was run in solvent free conditions at 40 °C. <sup>b</sup> The products were identified by comparison with authentic sample retention times using GC analysis and NMR spectra. The yields of reactions were obtained using GC analysis. <sup>c</sup> The selectivities of the products were >99% based on GC analysis.

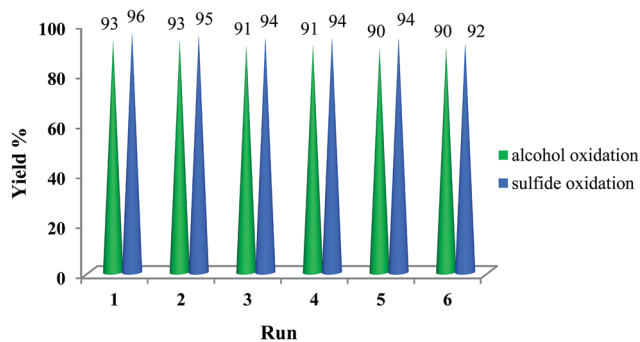


Fig. 9 Recycling of the catalytic system for the oxidation of 4-chlorobenzyl alcohol and thioanisole using the Ni(II)Rf<sub>2</sub> nanocomplex, according to procedures mentioned in the Experimental section.

using the title nanocatalyst, and is shown in Scheme 3. In this context, Lewis acid activation of the peroxide is the key intermediate in the oxidation of sulfides.<sup>52,53</sup>

In Table 3, the oxidative activity of other Ni based catalysts is compared with Ni(II)Rf<sub>2</sub> in the oxidation of benzyl alcohol and thioanisole. Compared to these previously reported methods,

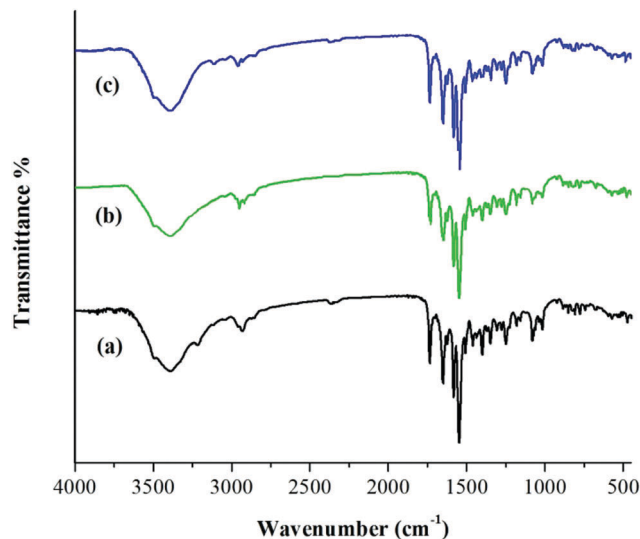
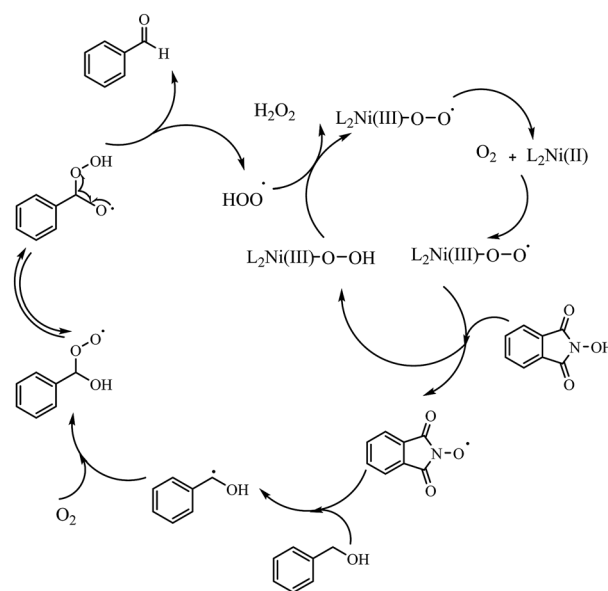
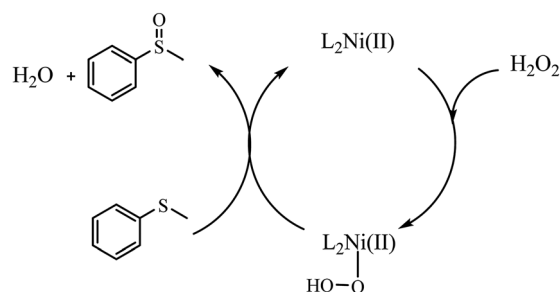


Fig. 10 FT-IR spectra of the fresh Ni(II)Rf<sub>2</sub> nanocomplex (a) and after 6 cycles in the oxidation of 4-chlorobenzyl alcohol (b) and oxidation of thioanisole (c).



Scheme 2 A plausible mechanism for the aerobic oxidation of alcohols in the presence of the Ni-catalyst/NHPI system.



Scheme 3 A plausible mechanism for the oxidation of sulfides in the presence of the Ni-catalyst/H<sub>2</sub>O<sub>2</sub> system.

**Table 3** Comparison of the oxidative activity of Ni(II)Rf<sub>2</sub> with other Ni-based catalysts in the oxidation of benzyl alcohol and thioanisole

Entry	Catalyst	Catalyst (g)	Conditions	Time (h)	Yield (%)	Ref.
Benzyl alcohol						
1	Ni(II)Rf <sub>2</sub>	0.005	EtOAc/NHPI/air/70 °C	4	91	This work
2	Mn <sub>6</sub> Ni <sub>4</sub>	0.2	Toluene/O <sub>2</sub> /100 °C	1	89	54
3	Ni-Co/FDU-15	0.5	DMF/air/110 °C	7	67	55
4	Ni-Al-hydrotalcite	0.5	Toluene/O <sub>2</sub> /90 °C	6	98	56
5	CO <sub>3</sub> <sup>2-</sup> -Ni <sub>2</sub> MgAl-LDH	1	Toluene/O <sub>2</sub> /80 °C	8	99	57
6	Ni(II)DPDME	0.005	MeCN/IBA/O <sub>2</sub> /60 °C	1	33	58
7	Co-Ni ferrite	0.003	MeCN/TBHP/hν	6	18.9	59
8	Ni(OH) <sub>2</sub>	0.3	Toluene/O <sub>2</sub> /90 °C	1	98	60
Thioanisole						
9	Ni(II)Rf <sub>2</sub>	0.005	Solvent free/H <sub>2</sub> O <sub>2</sub> / 40 °C	1.3	100	This work
10	[Ni(L) <sub>2</sub> (NO <sub>3</sub> ) <sub>2</sub> ].H <sub>2</sub> O	0.04	MeCN/H <sub>2</sub> O <sub>2</sub> /TMAO/r.t.	1	92	61
11	Ni-salen-MCM-41	0.02	EtOH/UHP/r.t.	2.6	95	62
12	NiFe <sub>2</sub> O <sub>4</sub>	0.07	MeCN/H <sub>2</sub> O <sub>2</sub> /r.t.	2	90	63

the presented catalytic oxidation systems are attractive from the point of view of catalyst loading, solvent nature, reaction time and yield.

## 4. Conclusions

In summary, we have successfully synthesized a novel of Ni(II)Rf<sub>2</sub> nanocomplex, by incorporating riboflavin as a biocompatible molecule with Ni(OAc)<sub>2</sub> under ultrasonic agitation at room temperature. FT-IR, ICP-AES, TGA, TEM, EDX, UV-vis and elemental studies have been used to characterize the prepared nanocatalyst. As a heterogeneous system, the Ni(II)Rf<sub>2</sub> nanocatalyst efficiently oxidizes a wide range of benzyl alcohols to the corresponding carbonyl compounds by employing air as an ideal oxidant and ethyl acetate as a safe solvent. Also, this catalytic protocol is applicable for the mild oxidation of sulfides in the presence of hydrogen peroxide under solvent free conditions. Notably, the catalytic oxidation systems presented herein showed remarkable selectivity. The use of air and H<sub>2</sub>O<sub>2</sub> as green oxidants, the mild reaction media employed, and the reusability and recyclability of the catalyst are salient features of the present method from an environmental point of view, and render the catalyst amenable to be used in industrial applications. The catalytic system in the present method is expected to provide new tools to pave the way towards more sustainable transformations involving transition metal-catalyzed C-H bond functionalization.

## Conflicts of interest

There are no conflicts of interest to declare.

## Acknowledgements

Support for this work by Research Council of University of Birjand is highly appreciated. We also thank "Iran Science Elites Federation" for partial support of this work.

## References

- R. Asmatulu, G. Mul, H. Yu, J. H. Clark, X. Xu, N. Yeerxiati, N. Hyder, Y. Sun, J. C. Colmenares and E. Asmatulu, *et al.*, *Green photo-active nanomaterials: sustainable energy and environmental remediation*, Royal Society of Chemistry, 2015.
- R. S. Varma, *Green Chem.*, 2014, **16**, 2027–2041.
- R. Bhandari, R. Coppage and M. R. Knecht, *Catal. Sci. Technol.*, 2012, **2**, 256–266.
- S. W. Snyder, G. Petersen, G. Kraus, C. Negri, J. H. Clark, T. Ezeji, N. Qureshi, K. Magrini, S. Datta and S. Peretti, *et al.*, *Commercializing biobased products: Opportunities, challenges, benefits, and risks*, Royal Society of Chemistry, 2015.
- S. H. Oh, H. S. Rho, J. W. Lee, J. E. Lee, S. H. Youk, J. Chin and C. E. Song, *Angew. Chem., Int. Ed.*, 2008, **47**, 7872–7875.
- P. T. Anastas and M. M. Kirchhoff, *Acc. Chem. Res.*, 2002, **35**, 686–694.
- J. H. Clark, V. Budarin, F. E. I. Deswarte, J. J. E. Hardy, F. M. Kerton, A. J. Hunt, R. Luque, D. J. Macquarrie, K. Milkowski and A. Rodriguez, *et al.*, *Green Chem.*, 2006, **8**, 853–860.
- D. E. T. Pazmino, M. Winkler, A. Glieder and M. W. Fraaije, *J. Biotechnol.*, 2010, **146**, 9–24.
- J. P. Escalada, A. Pajares, J. Gianotti, A. Biasutti, S. Criado, P. Molina, W. Massad, F. Amat-Guerri and N. A. Garcia, *J. Hazard. Mater.*, 2011, **186**, 466–472.
- G. de Gonzalo and M. W. Fraaije, *ChemCatChem*, 2013, **5**, 403–415.
- W. G. Santos, R. S. Scurachio and D. R. Cardoso, *J. Photochem. Photobiol., A*, 2014, **293**, 32–39.
- J. R. Merkel and W. J. Nickerson, *Biochim. Biophys. Acta*, 1954, **14**, 303–311.
- S. Iwahana, H. Iida and E. Yashima, *Chem. – Eur. J.*, 2011, **17**, 8009–8013.
- J. M. Grippa, A. de Zawadzki, A. B. Grossi, L. H. Skibsted and D. R. Cardoso, *J. Agric. Food Chem.*, 2014, **62**, 1153–1158.
- S. Chaudhuri, S. Sardar, D. Bagchi, S. S. Singha, P. Lemmens and S. K. Pal, *J. Phys. Chem. A*, 2015, **119**, 4162–4169.
- C. N. Malele, J. Ray and W. E. Jones, *Polyhedron*, 2010, **29**, 749–756.
- W. Zielenkiewicz, I. V. Terekhova, M. Koźbiał and R. S. Kumeev, *J. Therm. Anal. Calorim.*, 2010, **101**, 595–600.



- 18 R. Blume, M. Hvecker, S. Zafeiratos, D. Techner, A. KnopGericke, R. Schlgl, L. Gregoratti, A. Barinov and M. Kiskinova, *Nanostructured Catalysts: Selective Oxidations*, The Royal Society of Chemistry, 2011, pp. 248–265.
- 19 J. Piera and J.-E. Bäckvall, *Angew. Chem., Int. Ed.*, 2008, **47**, 3506–3523.
- 20 F. Geilen, B. Engendahl, A. Harwardt, W. Marquardt, J. Klankermayer and W. Leitner, *Angew. Chem.*, 2010, **122**, 5642–5646.
- 21 Z. Guo, B. Liu, Q. Zhang, W. Deng, Y. Wang and Y. Yang, *Chem. Soc. Rev.*, 2014, **43**, 3480–3524.
- 22 T. Matsumoto, M. Ueno, N. Wang and S. Kobayashi, *Chem. – Asian J.*, 2008, **3**, 196–214.
- 23 M. Uyanik and K. Ishihara, *Chem. Commun.*, 2009, 2086–2099.
- 24 G. Tojo and M. I. Fernández, *Oxidation of alcohols to aldehydes and ketones: a guide to current common practice*, Springer Science & Business Media, 2006.
- 25 J.-D. Lou and Z.-N. Xu, *Tetrahedron Lett.*, 2002, **43**, 6095–6097.
- 26 R. J. K. Taylor, M. Reid, J. Foot and S. A. Raw, *Acc. Chem. Res.*, 2005, **38**, 851–869.
- 27 C. Parmeggiani and F. Cardona, *Green Chem.*, 2012, **14**, 547–564.
- 28 D. Lenoir, *Angew. Chem., Int. Ed.*, 2006, **45**, 3206–3210.
- 29 M. Zhang, C. Chen, W. Ma and J. Zhao, *Angew. Chem., Int. Ed.*, 2008, **47**, 9730–9733.
- 30 T. Punniyamurthy, S. Velusamy and J. Iqbal, *Chem. Rev.*, 2005, **105**, 2329–2364.
- 31 H. Tsunoyama, H. Sakurai, Y. Negishi and T. Tsukuda, *J. Am. Chem. Soc.*, 2005, **127**, 9374–9375.
- 32 S. K. Hanson, R. Wu and L. A. P. Silks, *Org. Lett.*, 2011, **13**, 1908–1911.
- 33 W. Partenheimer and V. V. Grushin, *Adv. Synth. Catal.*, 2001, **343**, 102–111.
- 34 N. Kakiuchi, Y. Maeda, T. Nishimura and S. Uemura, *J. Org. Chem.*, 2001, **66**, 6620–6625.
- 35 Y. Uozumi and R. Nakao, *Angew. Chem., Int. Ed.*, 2003, **42**, 194–197.
- 36 P. Zhang, Y. Gong, H. Li, Z. Chen and Y. Wang, *Nat. Commun.*, 2013, **4**, 1593–1603.
- 37 M. Jafarpour, A. Rezaeifard, M. Ghahramaninezhad and F. Feizpour, *Green Chem.*, 2015, **17**, 442–452.
- 38 R. Noyori, M. Aoki and K. Sato, *Chem. Commun.*, 2003, 1977–1986.
- 39 G. Grigoropoulou, J. H. Clark and J. A. Elings, *Green Chem.*, 2003, **5**, 1–7.
- 40 S. E. Martin and A. Garrone, *Tetrahedron Lett.*, 2003, **44**, 549–552.
- 41 A. Rezaeifard, R. Haddad, M. Jafarpour and M. Hakimi, *J. Am. Chem. Soc.*, 2013, **135**, 10036–10039.
- 42 M. Jafarpour, A. Rezaeifard, V. Yasinzadeh and H. Kargar, *RSC Adv.*, 2015, **5**, 38460–38469.
- 43 M. Jafarpour, H. Kargar and A. Rezaeifard, *RSC Adv.*, 2016, **6**, 25034–25046.
- 44 M. Jafarpour, F. Feizpour and A. Rezaeifard, *RSC Adv.*, 2016, **6**, 54649–54660.
- 45 M. Jafarpour, H. Kargar and A. Rezaeifard, *RSC Adv.*, 2016, **6**, 79085–79089.
- 46 M. Jafarpour, F. Feizpour and A. Rezaeifard, *Synlett*, 2017, 235–238.
- 47 M. Jafarpour, A. Rezaeifard and F. Feizpour, *ChemistrySelect*, 2017, **2**, 2901–2909.
- 48 M. S. Refat, M. A. A. Moussa and S. F. Mohamed, *J. Mol. Struct.*, 2011, **994**, 194–201.
- 49 F. Recupero and C. Punta, *Chem. Rev.*, 2007, **107**, 3800–3842.
- 50 Y. Ishii, S. Sakaguchi and T. Iwahama, *Adv. Synth. Catal.*, 2001, **343**, 393–427.
- 51 A. Rezaeifard, A. Khoshyan, M. Jafarpour and M. Pourtahmasb, *RSC Adv.*, 2017, **7**, 15754–15761.
- 52 A. Ghorbani-Choghamarani, P. Moradi and B. Tahmasbi, *RSC Adv.*, 2016, **6**, 56458–56466.
- 53 A. Bayat, M. Shakourian-Fard, N. Ehyaei and M. M. Hashemi, *RSC Adv.*, 2014, **4**, 44274–44281.
- 54 Q. Tang, C. Wu, R. Qiao, Y. Chen and Y. Yang, *Appl. Catal., A*, 2011, **403**, 136–141.
- 55 X. Fu, S. Wu, Z. Li, X. Yang, X. Wang, L. Peng, J. Hu, Q. Huo, J. Guan and Q. Kan, *RSC Adv.*, 2016, **6**, 57507–57513.
- 56 B. M. Choudary, M. L. Kantam, A. Rahman, C. Reddy and K. K. Rao, *et al.*, *Angew. Chem., Int. Ed.*, 2001, **40**, 763–766.
- 57 W. Zhou, Q. Tao, J. Pan, J. Liu, J. Qian, M. He and Q. Chen, *J. Mol. Catal. A: Chem.*, 2016, **425**, 255–265.
- 58 C. Sun, B. Hu and Z. Liu, *Heteroat. Chem.*, 2012, **23**, 295–303.
- 59 J. Tong, Q. Zhang, L. Bo, L. Su and Q. Wang, *J. Sol-Gel Sci. Technol.*, 2015, **76**, 19–26.
- 60 H.-B. Ji, T.-T. Wang, M.-Y. Zhang, Q.-L. Chen and X.-N. Gao, *React. Kinet. Catal. Lett.*, 2007, **90**, 251–257.
- 61 A. N. Kharat, A. Bakhoda and T. Hajiashrafi, *J. Mol. Catal. A: Chem.*, 2010, **333**, 94–99.
- 62 M. Nikoorazm, A. Ghorbani-Choghamarani, H. Mahdavi and S. M. Esmaeili, *Microporous Mesoporous Mater.*, 2015, **211**, 174–181.
- 63 A. M. Kulkarni, U. V. Desai, K. S. Pandit, M. A. Kulkarni and P. P. Wadgaonkar, *RSC Adv.*, 2014, **4**, 36702–36707.